Neuron, Vol. 48, 109–121, October 6, 2005, Copyright ©2005 by Elsevier Inc. DOI 10.1016/j.neuron.2005.08.038

Modulation of Transmitter Release by Presynaptic Resting Potential and Background Calcium Levels

Gautam B. Awatramani, Gareth D. Price, and Laurence O. Trussell*
Oregon Hearing Research Center/Vollum Institute
Oregon Health & Science University
Portland, Oregon 97239

Summary

Activation of presynaptic ion channels alters the membrane potential of nerve terminals, leading to changes in transmitter release. To study the relationship between resting potential and exocytosis, we combined pre- and postsynaptic electrophysiological recordings with presynaptic Ca^{2+} measurements at the calyx of Held. Depolarization of the membrane potential to between –60 mV and –65 mV elicited P/Q-type Ca^{2+} currents of < 1 pA and increased intraterminal Ca^{2+} by < 100 nM. These small Ca^{2+} elevations were sufficient to enhance the probability of transmitter release up to 2-fold, with no effect on the readily releasable pool of vesicles. Moreover, the effects of mild depolarization on release had slow kinetics and were abolished by 1 mM intraterminal EGTA, suggesting that Ca^{2+} acted through a high-affinity binding site. Together, these studies suggest that control of resting potential is a powerful means for regulating synaptic function at mammalian synapses.

Introduction

Accumulation of Ca^{2+} in presynaptic nerve terminals both triggers and modulates the release of transmitters. Ca^{2+} buildup may occur during presynaptic nerve activity and lead to various forms of plasticity that are typically characterized by their lifespan, such as facilitation and potentiation (Zucker and Regehr, 2002). Additionally, Ca^{2+} may rise following activation of presynaptic receptors and channels (MacDermott et al., 1999). Ionotropic receptors, such as nicotinic, kainate, or ATP receptors, enhance release, possibly because of the high Ca^{2+} permeability of their associated ion channels (MacDermott et al., 1999). In addition, $GABA_A$ and glycine receptors weakly depolarize the presynaptic terminals, increase intraterminal calcium, and facilitate release at some synapses (Jang et al., 2002; Turecek and Trussell, 2001, 2002; Ye et al., 2004).

It is not known how a small depolarization can increase intraterminal Ca^{2+}. This is particularly perplexing because Ca^{2+} channels in the calyx of Held, where such presynaptic receptors have been described (Turecek and Trussell, 2001, 2002), are thought to require depolarization positive to –45 mV for their activation, far higher than that achieved by receptor activation (<–55 mV). Indeed, synaptic facilitation, mediated by Ca^{2+} accumulation, is achieved by conditioning depolarizations to –30 mV or more (Felmy et al., 2003). These studies suggest that the facilitating effects of small depolarizations may be mediated by pathways other than Ca^{2+} channels, such as activation of Ca^{2+} transporters or intracellular Ca^{2+} release mechanisms. Identifying the mechanisms of such modulation is important to the understanding of all depolarizing presynaptic receptors, highlighting the significance of ion channels that determine the resting potential of a presynaptic terminal.

In this study, we explored the link between the resting potential, Ca^{2+}, and exocytosis in the calyx of Held. Elevation of resting potential between –80 and –60 mV led to activation of P/Q-type Ca^{2+} channels, a gradual rise in the background level of Ca^{2+}, and a 2-fold increase in the amplitude of the glutamatergic EPSC. Neither the depolarization nor this small change in Ca^{2+} (50–100 nM) altered the spike-evoked Ca^{2+} influx, yet they were sufficient to increase significantly the probability of glutamate release. Thus, presynaptic Ca^{2+} channels serve to control release in two ways: the rapid activation and deactivation of the channels mediates phasic exocytosis, while their sensitivity to resting potential alters ambient Ca^{2+} levels and thus controls release probability.

Results

Small Depolarization-Dependent Enhancement of EPSCs Is Ca^{2+} Dependent

Simultaneous pre- and postsynaptic recordings were employed to probe the relationship between the membrane potential preceding a nerve terminal action potential and the glutamate release evoked by it. Release of glutamate was monitored by AMPA receptor-mediated currents in postsynaptic neurons. When the presynaptic membrane potential was slowly shifted positive from rest (~–80 mV) for 10 s, the peak amplitude of the subsequent spike-evoked EPSC increased (Figure 1A). This small depolarization-dependent enhancement, termed SDE, was evident when the presynaptic membrane potential was changed by as little as 10 mV. (We have used the term SDE here in order to distinguish this phenomenon from conventional facilitation or augmentation of synaptic strength). When potentials were raised to values near –60 mV, the EPSC was enhanced up to 2-fold (Figures 1A and 1B). Membrane potentials more depolarized than –60 mV produced variable effects on the EPSC, either increasing or decreasing it in different terminals, presumably as a consequence of facilitation of exocytosis; inactivation of K^+, Na^+, and Ca^{2+} channels (Figure 2C); and distortion of the action potential waveform (data not shown). However, at potentials negative to –60 mV, spike size and shape were not significantly altered ($p = 0.88$ and 0.16, for height and width of spikes at –80 mV and –60 mV, respectively), despite the change in EPSC (Turecek and Trussell, 2001; Kaneko and Takahashi, 2004, see also Figures 6C and 7C). Thus, modest changes in resting potential have a strong impact on release properties of calyceal terminals.

*Correspondence: trussell@ohsu.edu

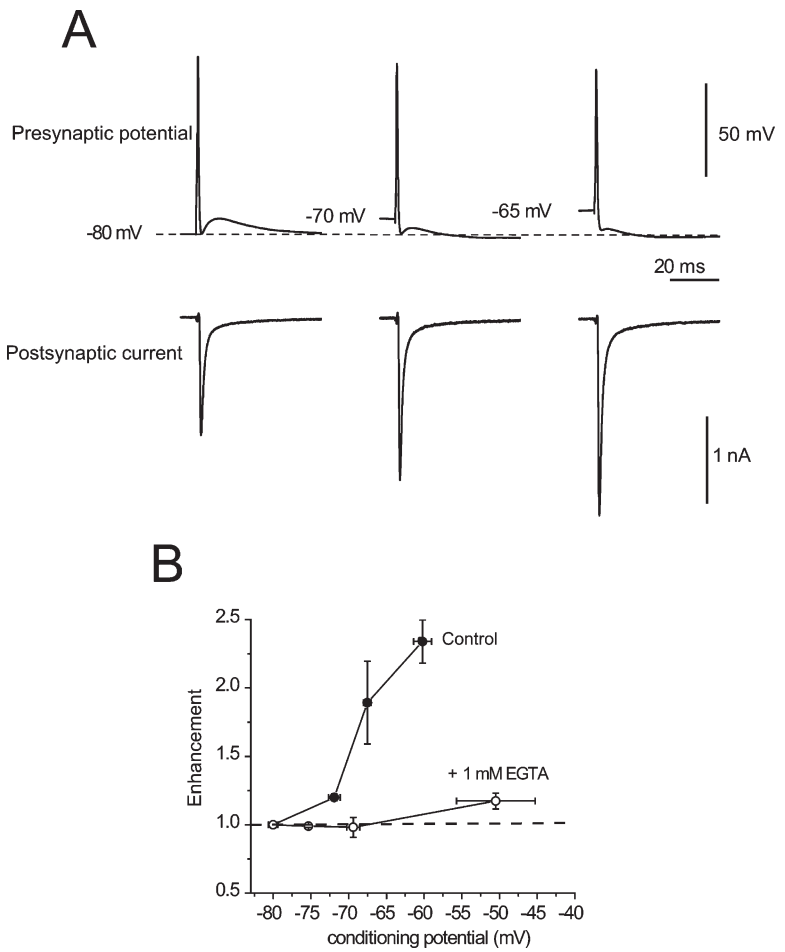

Figure 1. Depolarization-Induced Enhancement of EPSCs Is Ca^{2+}-Dependent

(A) Dual recordings of presynaptic membrane potential (upper traces) and postsynaptic current (lower traces). Presynaptic spikes were triggered by 1 ms 2 nA pulses. The membrane potential preceding the pulse was adjusted to the indicated final value for 10 s.

(B) Relation between the fold enhancement of the EPSC and the membrane potential just prior to the spike. Filled circles indicate data for six recordings with 25 μM fura-2 or BAPTA as the added buffer in the presynaptic patch-pipette (as in [A]). Open circles show data for five 5 cells in which 1 mM EGTA plus 25 μM BAPTA were in the presynaptic pipette. Note that the concentration of "fast" buffer (BAPTA or fura-2) was not changed in these experiments. Error bars indicate ±SEM.

In the presynaptic recordings described so far, patch-pipettes contained a low concentration of BAPTA or fura-2 (25 μM) to minimize competition with endogenous buffering mechanisms (Borst et al., 1995; Helmchen et al., 1997). At these concentrations, BAPTA does not interfere with the release process (Borst et al., 1995). To test directly the involvement of Ca^{2+} in SDE, 25 μM BAPTA + 1 mM EGTA were loaded into terminals. Owing to its slow kinetics and high affinity, EGTA at this concentration buffers global Ca^{2+} without preventing transmitter release (Borst and Sakmann, 1996). In experiments in which the buffering capacity was increased, the EPSC was no longer affected by depolarization over this same range of membrane potentials (Figure 1B). These findings therefore provide a causal link for increases in global Ca^{+2} and SDE.

Conditioning Depolarizations Increase Release Probability Downstream of Ca^{2+} Channels

In order to determine which aspects of transmission are altered by depolarization, we examined the effect of preconditioning potentials on the amplitude of the Ca^{2+} current evoked by a brief, action potential-like voltage pulse (Figure 2). Previous studies showed that large preconditioning pulses led to Ca^{2+} current facilitation, which may be dependent on Ca^{2+} influx (Borst and Sakmann, 1998; Cuttle et al., 1998). Indeed, pairs of brief pulses did result in acceleration of the rising phase and an increase in the peak amplitude of Ca^{2+} current in our experiments (Figure 2A). However, 5 s changes in the membrane potential to between –80 mV and –60 mV prior to a brief, strong voltage pulse had no significant effect on the Ca^{2+} current (Figures 2B and 2C). In two of eight cells tested, the Ca^{2+} currents showed a small facilitation (~7.5%) after predepolarizations to –55 mV (greater depolarization than that used for SDE). However, in the remaining cells, conditioning potentials to –50 mV significantly inhibited the Ca^{2+} current (6% ± 3%; $n = 6$, $p < 0.05$), presumably due to inactivation of Ca^{2+} current during the prepulse (Figures 2B and 2C) (Forsythe et al., 1998). Thus, SDE cannot be due to enhancement of the Ca^{2+} current, but instead must result from a process downstream of Ca^{2+} entry.

Such downstream actions could include effects on the vesicle release probability or vesicle pool size. Paired-pulse plasticity of EPSCs, a monitor of changes in release probability, was examined by delivering two stimuli to the calyx at 10 ms intervals and measuring the ratio of the amplitudes of the resulting EPSCs. The membrane potential before the first of the EPSCs was set to either –80 mV (gray trace) or –60 mV (black trace) for 10 s. With a prepotential of –80 mV, the EPSCs ex-

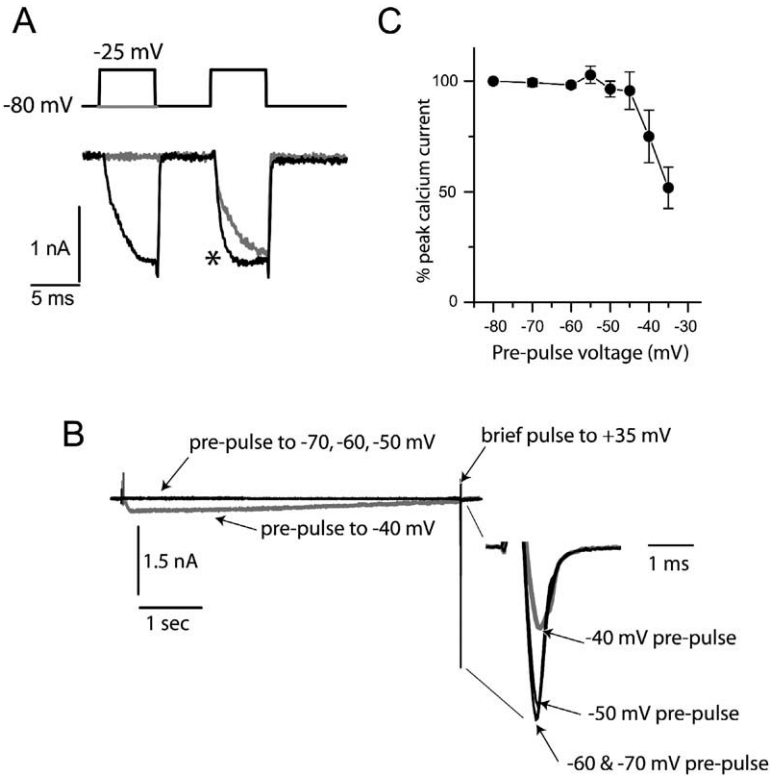

Figure 2. Predepolarization Does Not Enhance Ca^{2+} Current

(A) Demonstration of prepulse facilitation of Ca^{2+} current in the calyx (Borst and Sakmann, 1998; Cuttle et al., 1998). The rise time of a response to a brief pulse to –25 mV is accelerated by a 5 s pulse delivered just beforehand (black trace). A single pulse is shown in gray.

(B) A 0.5 ms pulse to +35 mV was used to evoke a Ca^{2+} tail current. This was preceded by 5 s steps to the indicated potentials (between –70 and –40 mV). None of the preceding steps led to potentiation of the Ca^{2+} tail current, and the step to –40 mV (in gray) both activated Ca^{2+} current and led to reduction in the tail current. Data in (A) and (B) are from the same recording.

(C) Normalized amplitude of the tail current as a function of prepulse potential for eight calyces. Error bars indicate ±SEM.

hibited a facilitation (the ratio of the second to the first EPSC in the pair) of about 50% (Figures 3A and 3B). In contrast, a prepotential of –60 mV increased the first EPSC more than the second. On average, the paired-pulse ratio was significantly reduced from 1.56 ± 0.11 to 1.11 ± 0.07 ($p < 0.05$; $n = 6$). These data suggest that the change in presynaptic membrane potential increased the probability of transmitter release.

In the calyx, Ca^{2+} is known to be involved in the recruitment of vesicles to the readily releasable pool (RRP) (Sakaba and Neher, 2001a; Wang and Kaczmarek, 1998); moreover, the RRP may be augmented by submicromolar increases in $[Ca^{2+}]$ observed during posttetanic potentiation or PTP (Habets and Borst, 2005). Therefore, we next looked at the effect of the preconditioning steps on the size of the RRP. Recordings were made from five presynaptic-postsynaptic pairs in the presence of 5 mM kynurenate and 100 μM cyclothiazide to attenuate receptor saturation and desensitization (Sakaba and Neher, 2001b; Wu and Borst, 1999). As shown in Figure 3C, brief (0.8–1.5 ms) pulses to 0 mV applied to calyces induced small Ca^{2+} currents (mean charge = 0.83 ± 0.06 pC) and small EPSCs (mean amplitude = –564 ± 130 pA). After depolarizing the calyces to –60 mV for 5 s, identical brief depolarizing pulses to 0 mV induced Ca^{2+} currents the same size as control currents (0.78 ± 0.07 pC, $p > 0.08$, paired Student's t test). Nonetheless, these Ca^{2+} currents elicited significantly larger EPSCs (mean test EPSC = 811 ± 134 pA; 166% ± 20% of control EPSC, $p < 0.001$, paired Student's t test). When EPSCs were compared by charge rather than peak amplitude, test EPSCs were still significantly larger (control = 13.7 ± 3.2 pC; test = 20.4 ± 4.3 pC; $p < 0.05$, paired Student's t test). On average, the integral of the control EPSC was 5% of the integral of the EPSC elicited by a depleting pulse (see below). The average percent changes in Ca^{2+} charge or EPSC for brief pulses are summarized in Figure 3Ei. These data indicate that SDE occurs downstream of Ca^{2+} channels and also show that SDE does not depend on tiny changes in spike width, since the duration of the voltage pulse that triggers release was the same.

To determine whether the enhancement of the EPSCs was due to an increase in the RRP, we tested the same calyces with 20 ms pulses to 0 mV (Figures 3D and 3Ei). Such voltage pulses elicited large Ca^{2+} currents (17.9 ± 1.6 pC) and large EPSCs (mean charge = 297 ± 57 pC), which have previously been shown to be sufficient to deplete most of the RRP (Sakaba and Neher, 2001b; Wu and Borst, 1999). Following a 5 s depolarization of the calyces to –60 mV, a second 20 ms pulse to 0 mV elicited slightly smaller Ca^{2+} currents (16.5 ± 1.5 pC, $p < 0.01$, paired Student's t test). However, there was no change in the EPSC charge (286 ± 54 pC; 96.6% ± 1.7% of control EPSCs). Peak amplitudes were also not significantly different (control mean = 3.2 ± 0.55 nA; test mean = 3.2 ± 0.62 nA). These are summarized in Figure 3Ei. The ratio of the average postsynaptic responses to short and long voltage pulses provides an estimate of release probability; these were 4.7% and 7.3% for pulses from –80 mV and –60 mV, respectively (ratio of charge, $p < 0.01$, paired Student's t test; Figure 3Eii). Together, these data indicate that SDE results from an increase in the fraction of the vesicle pool that is released with each action potential, with no change in the vesicle RRP size.

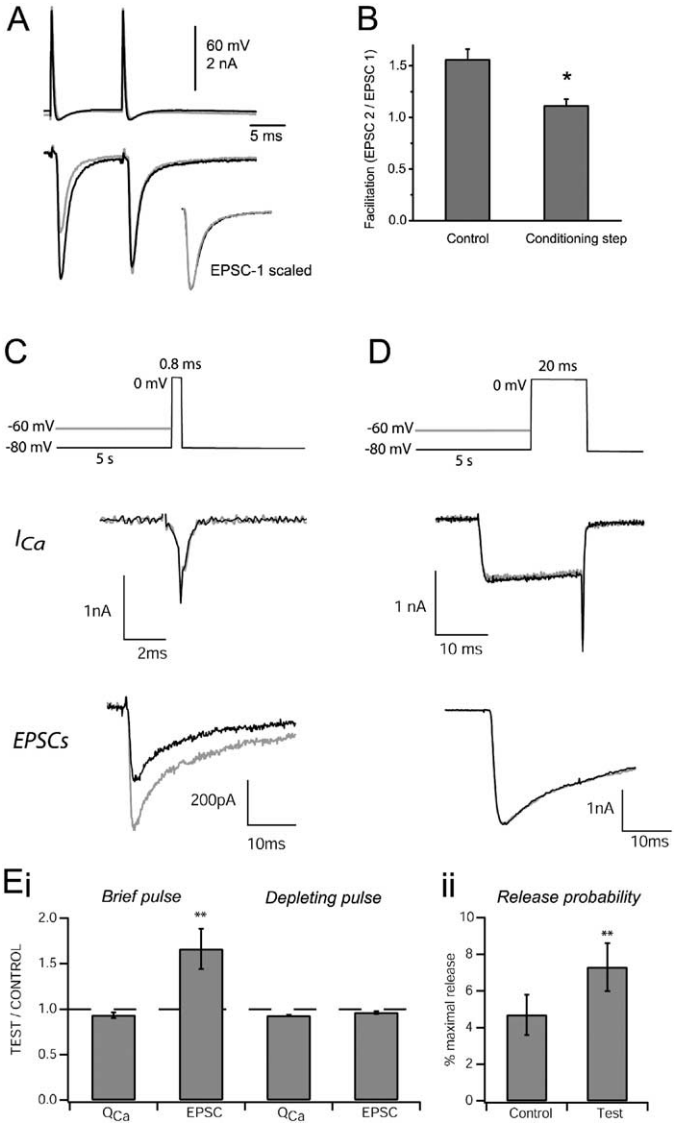

Figure 3. SDE Enhances Vesicle Release Probability Downstream of Ca^{2+} Channels

(A) Paired recording in which two calyceal spikes were triggered 10 ms apart. The resulting EPSCs exhibit facilitation when the potential preceding the spike was –80 mV (gray traces) and slight depression when the potential was depolarized by about 8 mV (black traces). Inset shows the first EPSC in the two conditions peak-scaled to illustrate that their time courses are identical.

(B) Average paired-pulse plasticity measured as the ratio of the second to the first EPSC in a pair. Comparisons made with spikes evoked from the resting potential of the terminal (–75 mV to –80 mV) (control) with pairs elicited after a depolarization of 8–10 mV. Significant difference from control: *$p < 0.018$ ($n = 6$ pairs). Error bars indicate ±SEM.

(C) Paired recordings of presynaptic Ca^{2+} current (I_{Ca}) and postsynaptic EPSCs. Presynaptic voltage command, as illustrated. Bath solutions included kynurenate and cyclothiazide (see Experimental Procedures). Presynaptic prepulse to –60 mV did not alter Ca^{2+} current, but increased EPSC compared to responses with prepulse of –80 mV.

(D) Same synapse as in (C), but releasing pulse was 20 ms instead of 0.8 ms. With use of this depleting stimulus, the prepulse value did not affect the amount of release.

(Ei) Average of ratios of responses to test (V_{hold} = –60) and control (V_{hold} = –80 mV). Shown are data from charge during Ca^{2+} current (Q_{Ca}) and peak synaptic current (EPSC). EPSC ratio is significantly greater than 1 (one-sample Student's t test, **$p < 0.05$). Error bars indicate ±SEM.

(Eii) Ratio of EPSC charge in response to brief and depleting voltage pulse for control and test V_{hold}. Ratios for test and control are significantly different: **$p < 0.01$ (paired Student's t test). Error bars indicate ±SEM.

Background Ca^{2+} Set by P/Q-Type Channels

Ca^{2+} concentration was measured using the indicator fura-2 in order to monitor the increase in average Ca^{2+} concentration across the terminal resulting from small depolarizations. Simultaneous measurement of Ca^{2+} concentration and Ca^{2+} current revealed that elevations of Ca^{2+} occurred at potentials at which we were unable to detect an inward current using a standard leak subtraction protocol (Figure 4A). Ca^{2+} current was most apparent when the depolarizing pulse reached values more positive than –50 mV (Figure 4A), consistent with findings in previous studies of calyceal Ca^{2+} current (Borst and Sakmann, 1998; Borst et al., 1995). However, a clear increase in Ca^{2+} was detected even at –65 mV. Figure 4B shows the relationship between [Ca^{2+}] and membrane potential, revealing that the change in Ca^{2+} associated with SDE was low, such that a 2-fold increase in EPSC occurred with an increase in Ca^{2+} of less than 50 nM. Nevertheless, this small rise in Ca^{2+} constitutes a substantial fractional increase when compared to the resting level of Ca^{2+} of the terminal (87 ± 16 nM, n = 6).

We then compared the rise and decay times of Ca^{2+} against the pulse voltage or peak Ca^{2+} for that voltage (Figures 4Ci and 4Cii). An average weighted time constant (τ_{wd}) was estimated by normalizing and integrating Ca^{2+} signals during their decay phases. In response to 2 s pulses to –60 mV (briefer than the pulses in experiments shown in Figures 6 and 7), the signals were slow to rise and decay (τ_{rise} = 0.9 ± 0.3 s; τ_{decay} = 0.9 ± 0.2 s), presumably due to an equilibration of Ca^{2+} influx and to buffering and extrusion mechanisms. With stronger depolarizations, which were associated with larger peak Ca^{2+} levels, the kinetics of both the onset and offset of the Ca^{2+} rise accelerated. Following pulses to –40 mV, Ca^{2+} decayed in two distinct phases, which could be estimated with double exponential functions (data not shown). Most of the Ca^{2+} increase at this voltage decayed quickly t_{fast} = 244 ± 24 ms (80% ± 8%), while the remaining decayed with t_{slow} =

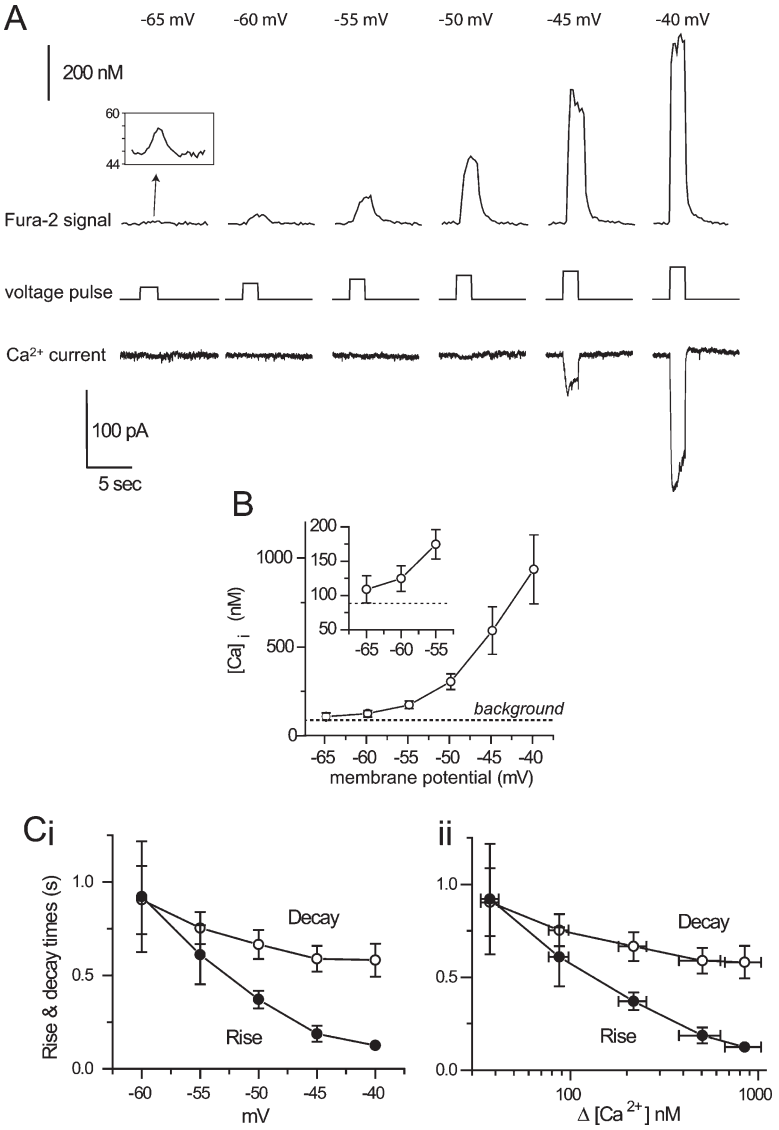

Figure 4. Voltage Dependence of Ca^{2+} Signals

(A) Single records of calibrated fura-2 signals, applied voltage pulses from –80 mV (as indicated at top of panel), and leak-subtracted Ca^{2+} currents. Ca^{2+} current became apparent at the –45 mV pulse, but Ca^{2+} signals were present even at –65 mV. Inset shows an average of three sweeps, filtered with a 5-point boxcar filter for the pulse to –65 mV on an expanded vertical scale.

(B) Absolute Ca^{2+} levels before ("background") and during voltage pulses for six calyces. (C, Ci, and Cii) Time course of Ca^{2+} signals as functions of voltage (Ci) or peak Ca^{2+} level (Cii). (Ci) 2 s pulses were made from –80 mV to between –60 mV and –40 mV, and the time constants of rise and decay of the Ca^{2+} signal were determined. These weighted time constants were then plotted against the potential of the pulse. (Cii) The same data is plotted as a function of the peak Ca^{2+} attained during the pulse. Error bars indicate ±SEM.

2559 ± 816 ms. It should be noted however, that the fast phases were probably overestimated due to the low sampling frequency of the optical measurement (4 Hz). Thus, Ca^{2+} changes quite slowly when triggered by potentials more hyperpolarized than those normally associated with evoked transmission and facilitation in this synapse (Bollmann et al., 2000; Felmy et al., 2003; Schneggenburger and Neher, 2000; see Discussion).

It is possible that extremely small Ca^{2+} currents, below the noise level of the previous experiments, could account for the Ca^{2+} increment that we have detected. To address this, we adopted a different protocol for revealing Ca^{2+} currents in which a slow voltage ramp from –90 to –40 mV was applied to the terminal (see Experimental Procedures). This was repeated in a solution containing Cd^{2+} and Ni^{2+} to block Ca^{2+} currents and the resulting traces were substracted. Figure 5A shows that at –65 mV, a Cd^{2+}/Ni^{2+}-sensitive inward current of ~0.3 pA was activated, suggesting that a Ca^{2+} entry through voltage-sensitive Ca^{2+} channels is indeed the source of the Ca^{2+} increment at such negative potentials. That these small currents could in fact account for the Ca^{2+} rise is consistent with theoretical estimates. At steady state, Ca^{2+} entry and extrusion are in balance such that

$$I_{Ca}^{2+} = -2FV\gamma[Ca^{2+}]_i \quad (1)$$

where I_{Ca}^{2+} is the Ca^{2+} current, F is the Faraday constant, V is the calyx volume (Helmchen et al., 1997), γ is the extrusion rate, and $[Ca^{2+}]_i$ is the increment in free Ca^{2+}. Using our Ca^{2+} measurements and an estimate for γ of 400/s (Helmchen et al., 1997) gives predicted values of I_{Ca} at –65 mV and –60 mV of –0.50 ± 0.59 pA and –0.97 ± 0.56 pA, respectively, only slightly higher than those in our measurements. As shown below, overestimates of γ could account for this difference.

To ensure that a weak depolarization can increase Ca^{2+} via the presynaptic Ca^{2+} channels, we applied ω-agatoxin, a selective antagonist of the P/Q-type Ca^{2+}

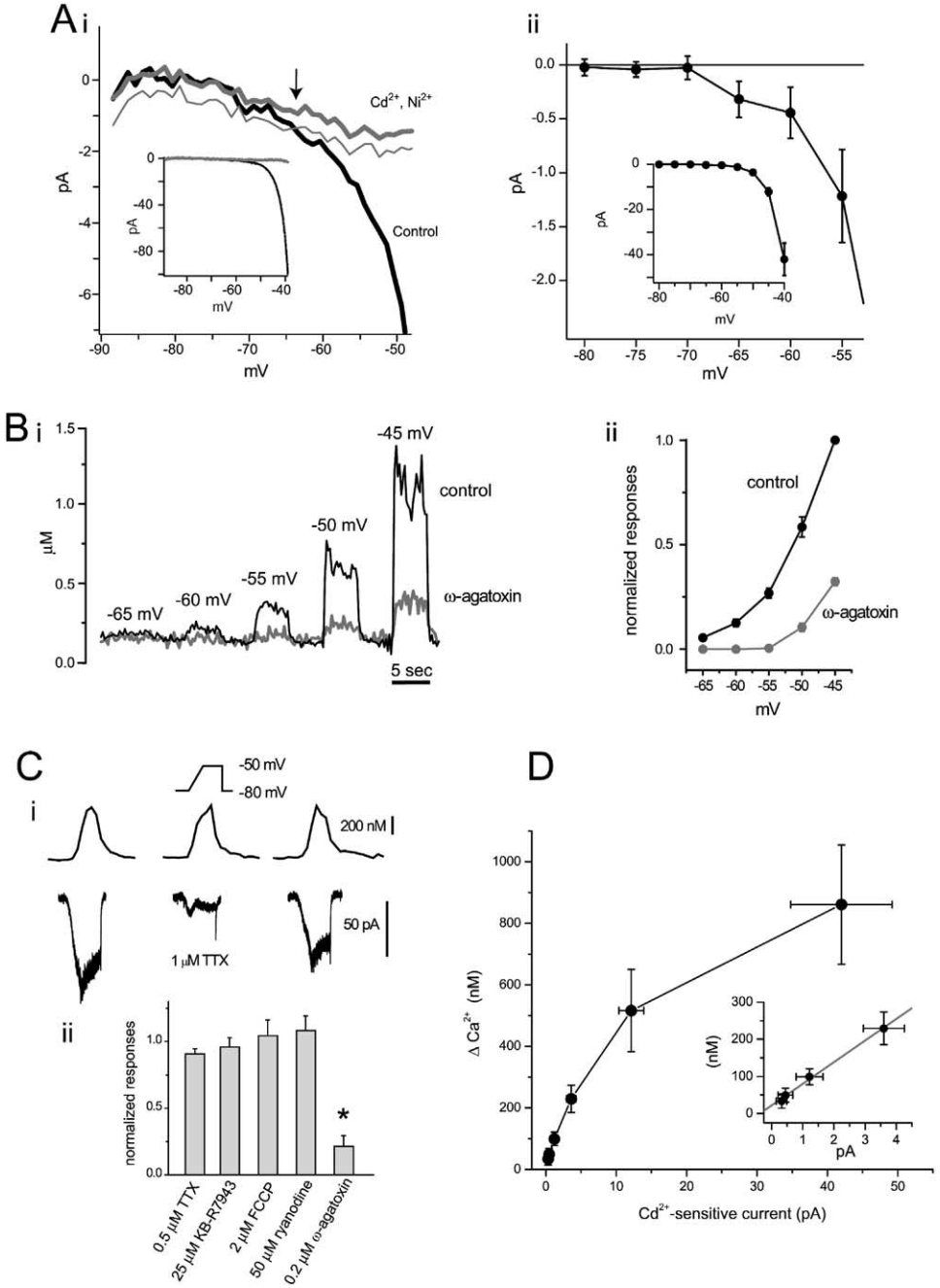

Figure 5. Ca^{2+} Signals during Small Voltage Pulses Result from Influx through P/Q-type Ca^{2+} Channels

(Ai) Ca^{2+} currents recorded in one terminal during a slow voltage ramp (17 mV/s) from –90 mV to –40 mV. Averages of 10 sweeps. Black trace indicates control; gray trace indicates application of 400 μM Cd^{2+} and 500 μM Ni^{2+} to block Ca^{2+} current. Main panel shows expanded view of the full record shown as an inset. Thin line shows –2 SD of the current noise. This –2 SD line shows where the control data exceed 2 SD of the trace in channel blockers, indicated by an arrow at –64 mV. (Aii) Averaged data from six to ten calyces. Inset: Mean Ca^{2+} current amplitudes at voltages between –90 and –40mV. Main panel: Expanded view of inset showing a detectable Ca^{2+} current at –65mV. (Bi) Ca^{2+} signals in response to pulses to the indicated potentials. Black lines, control solutions. Gray lines, bath-applied 200 nM ω-agatoxin. (Bii) Average data for effect of ω-agatoxin on four calyces.

(Ci) 5 s ramp steps from –80 mV to –50 mV elicit a TTX-sensitive inward current. TTX did not block the Ca^{2+} signal recorded simultaneously, suggesting that Na^{+}/Ca^{2+} exchange does not generate the Ca^{2+} signal. (Cii) Ca^{2+} signals after application of TTX (n = 4), KB-R7943 (n = 3), FCCP (n = 3), ryanodine (n = 3), and ω-agatoxin (n = 4). Ca^{2+} signals were normalized to the amplitude of the signal prior to drug application.

(D) Relationship between Ca^{2+} current in Figure 5Aii and Ca^{2+} increase derived from Figure 4B (peak – control) measured between –65 mV and –40 mV. Data plotted for estimates at each voltage. Inset: At lower end of the graph, Ca^{2+} levels and Ca^{2+} current are linearly related with a slope of 58 nM/pA (r = 0.99). Error bars represent ± SEM.

channels expressed in the calyx (Iwasaki and Takahashi, 1998). Indeed, ω-agatoxin (200 nM) significantly reduced the amplitude of the Ca^{2+} signal, especially at more negative potentials (Figure 5B). The apparent failure to completely block the Ca^{2+} rise at −45 mV may be due to the activation of the other types of voltage-sensitive Ca^{2+} channels that are found in the calyx (Iwasaki and Takahashi, 1998; Wu et al., 1998). In addition, we explored whether Na^+/Ca^+ exchange might contribute to a Ca^{2+} rise with small depolarizations. Voltage ramps from −80 mV to −50 mV for 5 s evoked an inward current that was blocked by TTX, suggesting the presence of a significant steady-state Na^+ current in the calyx or nearby axon (Figure 5Ci). Blockade of this current did not, however, alter the Ca^{2+} signal (Figure 5Ci), suggesting that Na^+ accumulation does not drive Na^+/Ca^+ exchange in reverse mode. This was confirmed by the lack of effect of KB-R7943, a blocker of exchange activity (Figure 5Cii). Moreover, disruption of mitochondrial potential with FCCP or of ryanodine receptors with ryanodine did not inhibit the Ca^{2+} signal (Figure 5Cii), suggesting that ER or mitochondrial stores do not contribute to the rise in Ca^{2+} that is triggered by a small depolarization.

Finally, we compared the Ca^{2+} increment to the Cd^{2+}/Ni^{2+}-sensitive current at each potential (Figure 5D). At the most negative potentials, this relationship was linear (Figure 5D, inset), consistent with an absence of Ca^{2+}-induced Ca^{2+} release playing a role in the Ca^{2+} rise. The slope of this relation can be used to estimate an extrusion rate according to equation 1, and gave a value of 222/s. This value is almost half that estimated from spike-induced rises in calyceal Ca^{2+}, as expected if extrusion rates vary with the Ca^{2+} load (Kim et al., 2005). An increase in extrusion rate with Ca^{2+} load would also explain why the slope of the relation in Figure 5D is lower for the larger voltage pulses, and why ω-agatoxin appears less effective at more depolarized potentials (Figure 5B). Taken together, these data support the hypothesis that even at potentials below the classical range for activation of these presynaptic Ca^{2+} channels, weak channel activation can occur, which, over seconds, leads to a new level of background Ca^{2+} in the nerve terminal and an alteration in synaptic strength.

Time Course of SDE

Because we can only measure the average Ca^{2+} concentration over the whole calyx, our estimates of the Ca^{2+} change associated with SDE may be erroneous if there is a substantial gradient in Ca^{2+} from the active zone to the outer face of the synapse. If so, the level of Ca^{2+} needed to induce SDE may be much larger than 50 nM. We reasoned that if enhancement required a low-affinity interaction with a Ca^{2+} sensor, driven by high, microdomain Ca^{2+}, then the synaptic enhancement should activate and terminate quickly, on the timescale of milliseconds, as the gradient forms and collapses. To test this hypothesis, the decay time of enhancement and Ca^{2+} were examined following termination of a small depolarizing current pulse. In Figure 6A a small 8 s current pulse was delivered, followed by a brief 2 nA pulse to trigger a spike; the corresponding EPSC is shown below. This protocol was repeated by varying the delay (Δt) between the end of the small pulse and the onset of the spike in order to track the decline of synaptic enhancement. The resulting family of sweeps is overlaid in Figure 6B. These show that the enhancement of the EPSC declined over several seconds. No change was seen in the width of the action potential, despite changes in EPSC amplitude (Figure 6C). The decline in the enhanced state lagged just behind the decay in Ca^{2+}, with average time constants of 1.7 and 3.7 s, respectively (Figure 6D). In these experiments, the predepolarization-evoked $[Ca^{2+}]$ decay was measured in separate trials to eliminate the contribution of large Ca^{2+} changes during spike activity. We used these data to examine the relationship between the low Ca^{2+} levels and the degree of EPSC enhancement. Figure 6E shows that Ca^{2+} and the fold enhancement of the EPSC by depolarization were linearly related, with a slope of 60 nM for a doubling of the EPSC from control. When plotted on a double-log scale (Figure 6E, inset), the EPSC varied with $[Ca^{2+}]^n$ with n = 1.09. Thus, enhancement of the EPSC by low Ca^{2+} levels occurs with less apparent cooperativity than with spike-triggered exocytosis (Borst and Sakmann, 1996).

Similarly, the onset of enhancement and the rise in $[Ca^{2+}]$ followed almost identical time courses to their decline (Figure 7). Here, a small current pulse was delivered for different durations, followed 10 ms later by a 2 nA, spike-triggering pulse (Figures 7A and 7B). The spike width was not affected by the duration of the predepolarization (Figure 7C). Over six cells, the time constant of the rising phase of $[Ca^{2+}]$ and EPSC enhancement was 2.1 and 3.4 s, respectively (Figure 7D). Together, these data show that ambient $[Ca^{2+}]$ changes slowly with alterations in resting potential, and this is followed by corresponding changes in synaptic strength. Moreover, the slow time course of change in EPSC amplitude argues against a steep gradient of resting $[Ca^{2+}]$ near the release sites, a conclusion supported by the ability of a slow Ca^{2+} buffer, EGTA, to eliminate the effect of changes in resting potential on EPSC amplitude (Figure 1B).

Discussion

Increased Ca^{2+} Causes SDE

Elevation of the membrane potential of calyceal nerve terminals between −80 and −60 mV caused an increase in the probability of transmitter release. Several lines of evidence suggest that this effect was mediated by alterations in ambient Ca^{2+} in the terminal. We showed that a small fraction of the high-voltage-activated P/Q-type Ca^{+2} channels may be open near the resting potential and mediate a small but potent rise in Ca^{2+}. In addition, intracellularly applied EGTA prevented SDE and, moreover, the slow changes in Ca^{2+} slightly preceded the time course of SDE of the EPSC. We have previously shown that an enhancement of the EPSC resulting from a small glycine-induced presynaptic depolarization is blocked by bath application of a membrane-permeant Ca^{2+} chelator and that the (glycine-

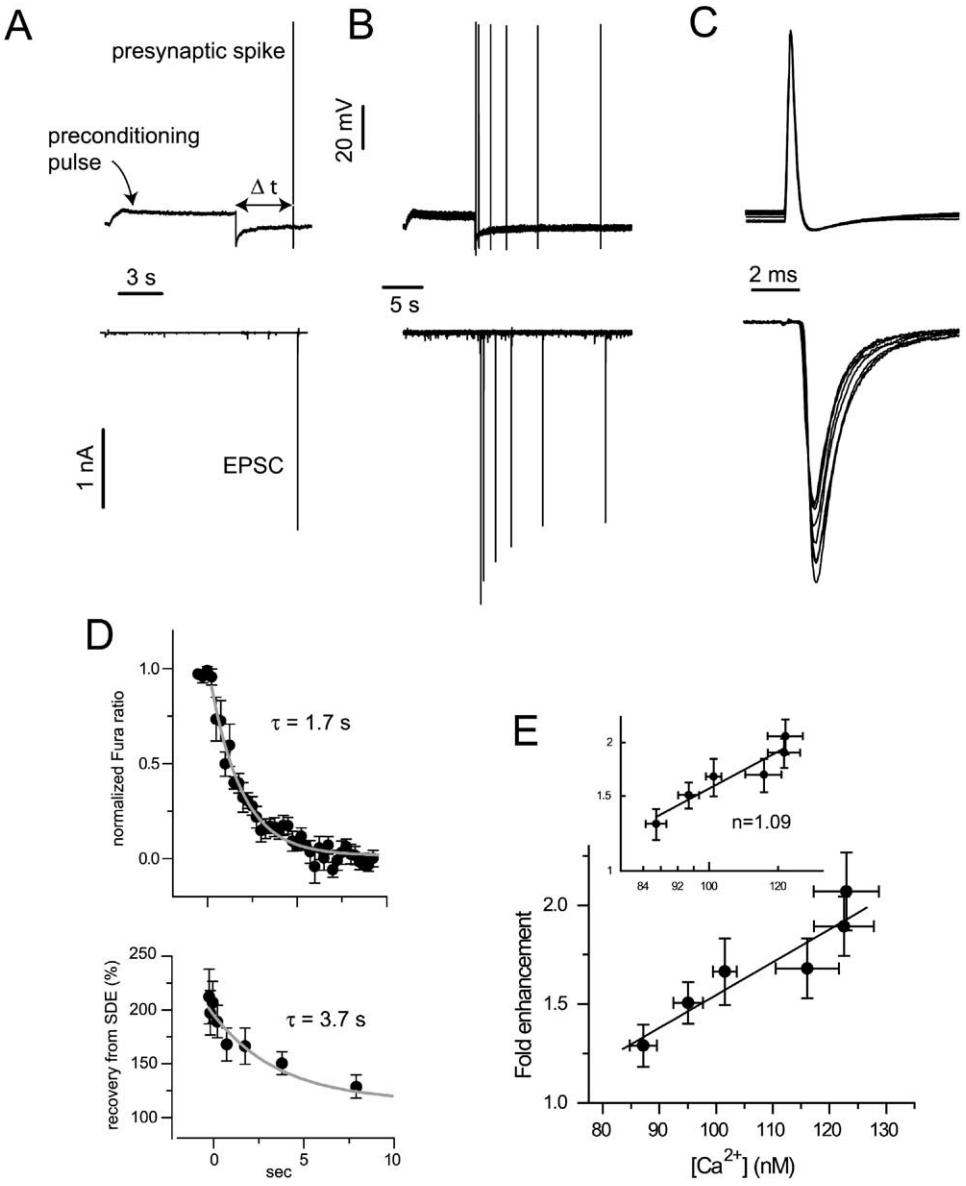

Figure 6. Decay of Ca^{2+} Rise and SDE

(A) Example of paired recording in which a presynaptic step was made from –80 mV to about –70 mV for 8 s. A spike was then triggered at a variable time (Δt) after return of the potential to –80 mV, resulting in an EPSC. (B) The protocol in (A) was repeated for different Δt values and the traces were overlaid to indicate the time for recovery of SDE. (C) Expanded view of presynaptic spikes (top) and EPSCs (bottom) for this experiment, indicating no change in the amplitude or width of the spikes. (D) Average decay time for Ca^{2+} signals (top, n = 7) and SDE of EPSCs (bottom, n = 9). Gray line is a single exponential fit with the time constant as shown. (E) The fold enhancement from SDE was compared to the Ca^{2+} level during their decay phases. SDE increased linearly with Ca^{2+} ($r = 0.95$, $p < 0.005$). Inset: Log-log plot of the data in (E) shows that EPSC enhancement increases with the 1.09 power of $[Ca^{2+}]$. Error bars indicate ± SEM.

mediated) increase in mEPSC frequency is blocked by Cd^{2+} (Turecek and Trussell, 2001) Together, these findings provide a strong link between resting potential, basal calcium, and synaptic strength.

Ca^{2+} Channel Activity at Hyperpolarized Potentials

The change of membrane potential that leads to SDE is within the range that results from glycinergic modulation in the calyx (Turecek and Trussell, 2001), suggesting that control of resting potential may be a powerful regulator of baseline synaptic strength. Yet, these membrane potential values are far below the apparent activation range of P/Q-type Ca^{2+} channels that has been previously reported (> –45 mV; Borst and Sakmann, 1998; Iwasaki and Takahashi, 1998; Wu et al., 1998). Our data suggest that very weak activation of channels, producing a current detectable only by heavily averaged, leak-subtracted whole-cell recordings, is still adequate to contribute to the ambient Ca^{2+} of the synapse (Figure 4). Felmy et al. (2003) found that steps to –26 mV

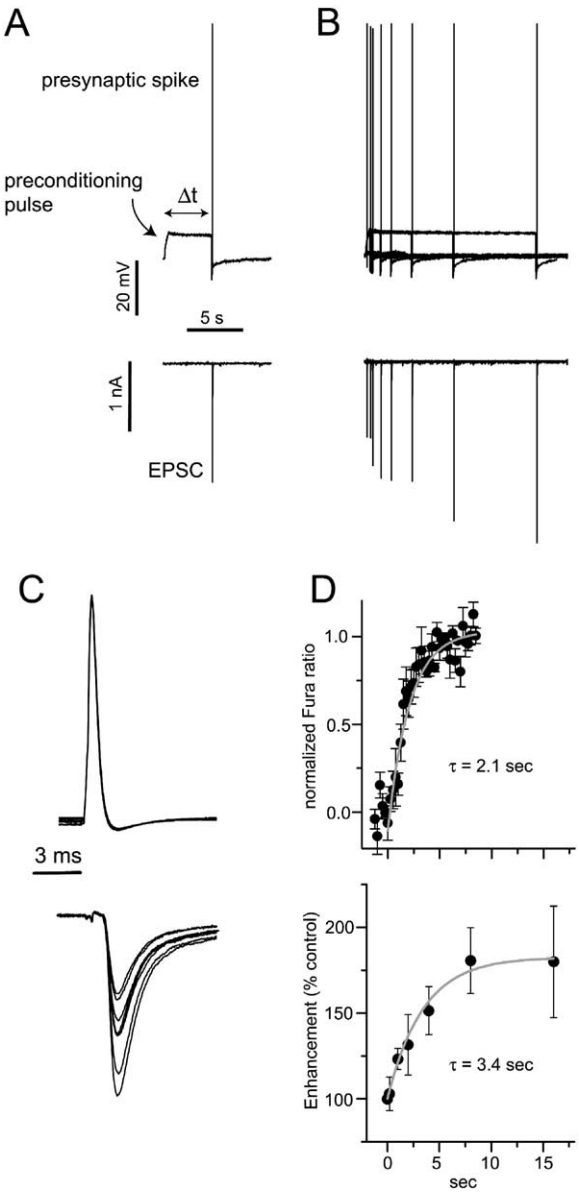

Figure 7. Onset of Ca^{2+} Rise and SDE

(A) Example of paired recording in which a presynaptic step was made from –80 mV to about –70 mV for a variable period of time (Δt). A spike was then triggered immediately after the step, resulting in an EPSC.

(B) The protocol in (A) was repeated for different Δt values, and the traces were overlaid to indicate the time course of onset of SDE.

(C) Expanded view of presynaptic spikes (top) and EPSCs (bottom) for this experiment, indicating no change in the amplitude or width of the spikes.

(D) Average decay time for Ca^{2+} signals (top, n = 7) and SDE of EPSCs (bottom, n = 9). Gray line represents a single exponential fit with the time constant as shown. Error bars indicate ±SEM.

were required to cause Ca^{2+}-dependent facilitation of release and Ca^{2+} rose to near micromolar levels. However, in those studies Ca^{2+} influx was elicited with brief (10–84 ms) depolarizing pulses. Here, we find that, at near-resting membrane voltages, Ca^{2+} rises with a $\tau \sim 1$ to 2 s, depending on the duration and intensity of the depolarization. Hence, by using longer pulses (5–10 s) of lower voltage, we reveal a small but functionally significant activation of P/Q-type Ca^{2+} channels. These finding are also consistent with findings in sensory neurons of increase in Ca^{2+} levels with depolarizations below the apparent activation range of Ca^{2+} channels (Kobayashi and Tachibana, 1995; Charpak et al., 2001). Finally, we note that these results are consistent with the slow onset of glycine and $GABA_A$ receptor effects on glutamate release from the calyx, which is far slower than the onset of ionic currents mediated by these agents (Turecek and Trussell, 2001, 2002).

In contrast to the rapid decay of Ca^{2+} transients following an action potential (~100–150 ms; Helmchen et al., 1997), we found that the rate of change of Ca^{2+} in response to mild depolarizations is an order of magnitude slower (Figures 4C, 6, and 7). A fast decay phase only became apparent following stronger depolarizations that cause Ca^{2+} to rise by several 100 nM. Such a biphasic decay of Ca^{2+} is characteristic of systems that have multiple buffers and extrusion pathways, with unique kinetic properties and concentration dependence (Maeda et al., 1999). This idea is consistent with recent anatomical studies that describe strong expression of calretinin and parvalbumin in the calyx (Felmy and Schneggenburger, 2004). The slow kinetics of the rise and decay phases of small Ca^{2+} changes observed during SDE are consistent with the high-affinity and slow buffering properties of parvalbumin. The rate of extrusion/sequestration will also be concentration dependent, and for lower Ca^{2+} levels, fewer such mechanisms will play significant roles in clearance; indeed, a recent study showed that calyceal mitochondria only contribute to Ca^{2+} sequestration when Ca^{2+} reaches the μM range (Kim et al., 2005).

It is unlikely that depolarization triggers Ca^{2+} release from stores: small depolarizations elicited Ca^{2+} rises that were resistant to ryanodine or FCCP. Moreover, Ca^{2+} channel antagonists blocked the effects of depolarization. Thapsigargin did not affect the EPSC in basal conditions, suggesting that the stores are not sufficiently primed or are not linked to release (Chuhma and Ohmori, 2002). The initial Ca^{2+} rise was linearly related to the measured Ca^{2+} current, not supralinearly, as expected for Ca^{2+}-induced Ca^{2+} release. Thus, presynaptic Ca^{2+} channels may serve two distinct functions that different dramatically in timescale. Submillisecond activation and deactivation is needed to evoke and terminate transmitter release. By contrast, the weak sensitivity of these channels to voltage changes near rest controls synaptic strength over the time frame of seconds.

Mechanism of SDE

At some synapses, including the calyx of Held, the local saturation of fast buffers is proposed to underlie facilitation (Blatow et al., 2003; Felmy et al., 2003; Jackson and Redman, 2003). The level of Ca^{2+} that leads to SDE is more than an order of magnitude lower in concentration and slower in decay kinetics than that associated with facilitation in the calyx (Felmy et al., 2003). Unlike facilitation at the calyx, SDE decayed about 1 s more slowly than Ca^{2+} levels, suggesting a slower intrinsic

decay of about 1 s. The higher sensitivity of SDE to Ca^{2+} and the slower intrinsic decay of enhancement is more in keeping with an augmentation or posttetanic potentiation-like process than classical facilitation (Habets and Borst, 2005; Delaney and Tank, 1994; Kamiya and Zucker, 1994; Korogod et al., 2005; Regehr et al., 1994). Moreover, these observations argue against simple residual Ca^{2+} or buffer saturation models for SDE.

Preconditioning steps that caused enhancement of the EPSC did not affect Ca^{2+} channels, suggesting that Ca^{2+} may work downstream of its entry. Ca^{2+} plays a critical role in the priming of vesicles, and prolonged periods with several hundreds of nM Ca^{2+} were found to increase the RRP in chromaffin cells (Smith et al., 1998; Voets et al., 1999) and hippocampal cultures (Rosenmund et al., 2002), as well as in the calyx of Held (Habets and Borst, 2005). However, in our experiments, increases of less than 100 nM that caused a change in probability of release were insufficient to cause any significant change in vesicle pool size, thus ruling out this possibility. The sensitivity to EGTA and the slow onset and offset of both volume-averaged Ca^{2+} and EPSC enhancement argue against a mechanism whereby high concentration microdomains near the Ca^{2+} channel could activate a low-affinity sensor. Hence, our data support models that propose a distinct high-affinity sensor, different from either the Ca^{2+} channel or exocytosis trigger (Atluri and Regehr, 1996; Tang et al., 2000; Matveev et al., 2002; Yamada and Zucker, 1992; Zucker and Regehr, 2002). Since, in the calyx of Held, the Ca^{2+} channel and the release sensor are thought to be ~100 nm apart (Meinrenken et al., 2002), such a modulatory sensor may have slow association rates that would prevent saturation during brief surges of Ca^{2+} during an action potential (Regehr et al., 1994). In recent studies of posttetanic potentiation (PTP) in the calyx, potentiation by low Ca^{2+} levels could not be accounted for by a direct action on the exocytotic Ca^{2+} sensor unless its sensitivity were altered (Habets and Borst, 2005; Korogod et al., 2005; Lou et al., 2005). This might occur if Ca^{2+} triggered a second messenger-mediated process that could either enhance Ca^{2+} sensitivity or directly enhance the probability of vesicle fusion; this scenario would be consistent with a roughly 1 s lag between the Ca^{2+} rise and enhancement (Figures 6 and 7), consistent with synaptic potentiation at mossy fiber synapses (Brager et al., 2003; Regehr et al., 1994). Interestingly, a recent study (Lou et al., 2005) has shown that a phorbol ester may enhance release by altering the sensitivity of the release sensor. Additionally, this study showed that the release sensor could respond weakly to very low Ca^{2+} levels, with a cooperativity similar to that we observed for SDE. It is also of interest that the relationship between PTP and background Ca^{2+} is similar to our estimate of a 60 nM change for a doubling of response (Korogod et al., 2005; Habets and Borst, 2005), suggesting that PTP and SDE may work through a common mechanism.

Presynaptic Regulation at Other Synapses

Previous studies on nerve terminals have generated opposing views on the role of resting potential in synaptic strength. In principle, one might expect depolarization to reduce the size of the spike (through Na^+ channel inactivation) and to reduce Ca^{2+} current activation, as well as the driving force for Ca^{2+} flowing during the tail current on the falling edge of the spike. Accordingly, in the squid giant synapse, transmitter release is enhanced by preceding *hyperpolarizing* membrane currents (Bullock and Hagiwara, 1957; Takeuchi and Takeuchi, 1962). Similar results were reported for neuromuscular junctions (Dudel, 1971; Hubbard and Willis, 1968). However, in the squid giant synapse and in crayfish neuromuscular junctions, protracted, small depolarizations were reported to enhance transmitter release, over a time frame similar to that we observed for evoked release in the calyx (Charlton and Atwood, 1977; Wojtowicz and Atwood, 1984). Moreover, elevation of extracellular K^+ ions, which should also depolarize synapses, increases transmitter output at neuromuscular junctions (Matyushkin et al., 1995; Takeuchi and Takeuchi, 1961). Shapiro et al. (1980) showed that presynaptic depolarization to between –60 mV and –35 mV enhanced acetylcholine release in *Aplysia* and attributed this effect to inactivation of the K^+ current, which broadened the spike, and steady activation of Ca^{2+} current. Similarly, in leech neurons, presynaptic depolarization enhances IPSPs, possibly as a result of spike broadening (Nicholls and Wallace, 1978). We have found in a mammalian central nerve terminal that small but functionally significant Ca^{2+} currents may be activated at even more negative potentials than in invertebrates. Unlike synapses in *Aplysia* and leech, SDE was not associated with a change in the spike width (Figures 6C and 7C). Clearly, this effect must depend on the magnitude of the depolarization and the properties of the channels and Ca^{2+} buffer in any given synapse. Nevertheless, these results suggest that channels that control the resting potential of a terminal may play an important role in the control of transmitter release in all synapses.

Our results bear on how presynaptic ionotropic receptors control transmitter release. A classical model of presynaptic inhibition, primary afferent depolarization, occurs when presynaptic $GABA_A$ receptors strongly depolarize nerve terminals and prevent successful spike invasion (Cattaert and El Manira, 1999). However, weaker GABA action at these synapses has the opposite effect and strongly potentiates afferent transmission (Duchen, 1986), consistent with our observations in the calyx terminal. While $GABA_A$ and glycine receptors couple to anion channels, other receptors, such as neuronal nicotinic and ATP receptors, activate cation channels, allowing both Na^+ and Ca^{2+} entry and thereby enhance exocytosis (Khakh and Henderson, 2000; MacDermott et al., 1999). The present study suggests, that, regardless of the ionic permeability, these receptors may enhance release through a common mechanism.

Experimental Procedures

Slice Preparation

Coronal slices of brainstem were prepared from 9- to 12-day-old Wistar rats as previously described (Borst et al., 1995). Briefly, 200 μm thick sections were prepared in ice-cold artificial cerebrospinal fluid (ACSF) using a vibratome (VT1000S; Leica, Deerfield, IL). The ACSF used for slicing was composed of 125 mM NaCl, 25 mM

glucose, 2.5 mM KCl, 3.0 mM $MgCl_2$, 0.1 mM $CaCl_2$, 1.25 mM NaH_2PO_4, 25 mM $NaHCO_3$, 0.4 mM ascorbic acid, 3 mM *myo*-inositol, and 2 mM sodium pyruvate, and it was bubbled with 5% CO_2/95% O_2. Immediately after the slices were cut, they were incubated at 37°C for 30–60 min in normal ACSF (similar to the slicing solution, but the concentration of the divalent ions was changed to 1.0 mM $MgCl_2$ and 2.0 mM $CaCl_2$ and also contained 0.1 mM DL AP5, 0.001 strychnine, and 0.010 SR95531). Thereafter, they were stored at room temperature. Recordings were all obtained within ~4 hr of slicing.

Whole-Cell Recordings

When ready for use, slices were transferred to a recording chamber and were continually perfused with ACSF (2–4 ml/min) at room temperature. Calyces were viewed using a Zeiss Axioskop FS equipped with differential interference contrast optics and a 63× water-immersion objective (NA 0.9; Achroplan, Zeiss). Pipettes were pulled from thick-walled borosilicate glass capillaries (WPI) using a horizontal puller (P97; Sutter Instruments) and had open tip resistances of 3–5 MΩ and 1.5–3 MΩ for the pre- and postsynaptic recordings, respectively. Whole-cell current- and voltage-clamp recordings were made with a dual headstage Multiclamp 700B amplifier (Axon Instruments, Foster City, CA) at room temperature. In some experiments involving dual voltage-clamp recordings, Axopatch 200A and 200B amplifiers were utilized. For presynaptic current-clamp experiments, pipettes were filled with 115 mM K-gluconate, 0.1 mM K-glutamate, 20 mM KCl, 1 mM $MgCl_2$, 10 mM HEPES, 4 mM MgATP, 0.3 mM GTP, and 10 mM phosphocreatine (~290 mOsM; pH, 7.2 with KOH). Ca^{2+} was buffered with 0.025 mM fura-2, 0.025 mM BAPTA, or 1 mM EGTA + 0.025 mM BAPTA, as specified. The glutamate and fura-2 ejected from the pipette while approaching the calyx were washed out for a period of ~15 min after formation of a gigaohm seal, to reduce the nonspecific background fluorescence and activation of presynaptic metabotropic glutamate receptors. After rupturing the seals, the Ca^{2+} buffer was allowed to equilibrate for another ~15 min, during which time the access resistances stabilized to values between 6 MΩ and 25 MΩ. Thereafter, the bridge was balanced and pipette capacitance compensation was applied. Evoked responses measured in voltage-clamped principal neurons were made with pipettes filled with solution containing 150 mM CsCl, 5 mM EGTA, 1 mM $MgCl_2$, 10 mM HEPES, 2 mM ATP, 0.3 mM GTP, 10 mM phosphocreatine, and 5 mM QX 314 (~310 mOsM), and the pH was adjusted to 7.2 with CsOH. Series resistances (4–12 MΩ) were compensated by 75%–90% (lag, 3.7 kHz) and monitored during the course of the experiment by small hyperpolarizing steps in both pre- and postsynaptic recordings. Resting potential was determined in current clamp (zero holding current). Liquid junction potentials were measured for all solutions, and reported voltages are appropriately adjusted.

To measure presynaptic Ca^{2+} currents in response to voltage pulses, recording electrodes were filled with a solution that contained: 150 mM CsCl, 10 mM TEA-Cl, 1.0 mM $MgCl_2$, 10 mM HEPES, 10 mM Na_2 phosphocreatine, 4 mM MgATP, and 0.3 mM GTP (~310 mOsm; pH adjusted to 7.2 with CsOH). Fura-2 (0.025 mM) or 0.025 mM BAPTA was used to buffer Ca^{+2} as specified. L-glutamate (0.1 mM) was also added in experiments in which EPSCs were measured simultaneously. To block K^+ and Na^+ channels, 20 mM NaCl in the ACSF was replaced with TEA-Cl (20 mM), and 4-AP (100 μM) and TTX (0.5 μM) were also added. In experiments determining RRP, 100 μM cyclothiazide and 5 mM kynurenic acid were added to the ACSF to reduce desensitization and saturation of AMPA receptors, respectively. Signals were filtered at 5 kHz and sampled at 20 kHz.

To measure presynaptic Ca^{2+} currents in response to voltage ramps, an intracellular solution was used that contained: 140 mM Cs methanesulphonate, 10 mM TEA-Cl, 10 mM HEPES, 10 mM Na_2 phosphocreatine, 4 mM Mg ATP, 0.3 mM Tris GTP, 0.025 mM BAPTA, 0.1 mM glutamate, and 0.1 mM Lucifer yellow. Voltages were corrected for a measured liquid junction potential of 9 mV. TEA-Cl (20 mM) was added to the extracellular solution (replacing 20 mM NaCl) plus CsCl (1 mM), 4-aminopyridine (100 μM), and TTX (0.5–1 μM). Calyces were voltage clamped at –80 mV. To record Ca^{2+} currents, 3 s voltage ramps from –90mV to –40mV were applied every 10 to 15 s in control solution and in the presence of Cd^{2+} (400 μM) plus Ni^{2+} (500 μM); the Cd^{2+}/Ni^{2+} solution was applied by continuous pressure ejection from a patch-pipette placed approximately 20 μm from the calyx. Six to ten voltage ramps were applied in each condition and averaged. Currents were filtered at 1 kHz and sampled at 5 kHz. Any voltage drift was noted at the end of each recording and subtracted from the command voltage ramp; drift was always less than 4 mV and was negative. Currents may have activated at slightly more negative voltages than those we report if such drift arose late in the recording. The data were analyzed in the following manner: to correct for leakage current, for each individual record a straight line was fitted to the first 600 ms of the current record (corresponding to a ramp from –90 to –80mV), extended through the entire length of the record, and then subtracted from the current trace. Control currents and currents recorded in the presence of Cd^{2+}/Ni^{2+} were averaged. To reduce noise further, average current traces were reduced from the 15,000 sampled data points to 50 data points by binning the 300 consecutive points corresponding to each 1 mV of ramp and taking the mean of these 300 points. Finally the Ca^{2+} current was obtained by subtracting the current in Cd^{2+}/Ni^{2+} from the control current.

Fluorescent Measurements

After equilibration in the calyx, fura-2 was excited at 357 nm (isosbestic point) and 380 nm light generated by a Polychrome IV monochrometer (TILL Photonics, Germany). A 400 nm long-pass dichroic mirror and a 510/40 band-pass emission filter (Chroma, Rockingham, VT) were used to select the appropriate wavelengths for excitation and collection of fura-2 signals. Fluorescence was measured using an IMAGO Super-VGA cooled charge-coupled device (TILL Photonics, Germany), controlled with TillVision 4.0 software. Pixels on the CCD chip were binned (4 × 4) to reduce the effective readout noise of the camera. Pairs of images stimulated at 357 nm and 380 nm were acquired every 250 ms (exposure time 20–40 ms). Background fluorescence was measured from a region adjacent to the calyx. Signals were averaged over regions of interest selected by manually tracing around calyces, background subtracted, and then converted into $[Ca^{2+}]$ using standard methods (Grynkiewicz et al., 1985). In vivo calibration measurement of R_{min} and $R_{intermediate}$ were made with pipette solution containing 20 mM EGTA and 13.3 mM Ca-EGTA + 6.7 mM EGTA, respectively. R_{max} was measured by eliciting trains of action potentials at 100 Hz. These values were: R_{min} = 0.64 ± 0.02 (n = 3); $R_{intermediate}$ = 0.98 ± 0.01 (n = 3); and R_{max} = 2.01 ± 0.13 (n = 4). Using these values, the Kd of fura-2 was calculated as 279 nM (assuming that the Kd for EGTA was 145 nM) similar to that reported previously (Helmchen et al., 1997).

Fura-2 was obtained from Molecular Probes (Eugene, OR) and other chemicals were obtained from Sigma (St. Louis, MO).

Data Analysis

Pre- and postsynaptic responses were analyzed in Clampfit 9.2 (Axon Instruments, Foster City, CA).

Acknowledgments

We thank Drs. K. Delaney, C. Jahr, and V. Shahrezaei for comments on the manuscript. This work was supported by NIH grant DC04450.

Received: March 15, 2005
Revised: July 27, 2005
Accepted: August 31, 2005
Published: October 5, 2005

References

Atluri, P.P., and Regehr, W.G. (1996). Determinants of the time course of facilitation at the granule cell to Purkinje cell synapse. J. Neurosci. *16*, 5661–5671.

Blatow, M., Caputi, A., Burnashev, N., Monyer, H., and Rozov, A. (2003). Ca^{2+} buffer saturation underlies paired pulse facilitation in calbindin-D28k-containing terminals. Neuron *38*, 79–88.

Bollmann, J.H., Sakmann, B., and Borst, J.G. (2000). Calcium sensitivity of glutamate release in a calyx-type terminal. Science *289*, 953–957.

Borst, J.G., and Sakmann, B. (1996). Calcium influx and transmitter release in a fast CNS synapse. Nature *383*, 431–434.

Borst, J.G., and Sakmann, B. (1998). Facilitation of presynaptic calcium currents in the rat brainstem. J. Physiol. *513*, 149–155.

Borst, J.G., Helmchen, F., and Sakmann, B. (1995). Pre- and postsynaptic whole-cell recordings in the medial nucleus of the trapezoid body of the rat. J. Physiol. *489*, 825–840.

Brager, D.H., Cai, X., and Thompson, S.M. (2003). Activity-dependent activation of presynaptic protein kinase C mediates posttetanic potentiation. Nat. Neurosci. *6*, 551–552.

Bullock, T.H., and Hagiwara, S. (1957). Intracellular recording from the giant synapse of the squid. J. Gen. Physiol. *40*, 565–577.

Cattaert, D., and El Manira, A. (1999). Shunting versus inactivation: analysis of presynaptic inhibitory mechanisms in primary afferents of the crayfish. J. Neurosci. *19*, 6079–6089.

Charlton, M.P., and Atwood, H.L. (1977). Modulation of transmitter release by intracellular sodium in squid giant synapse. Brain Res. *134*, 367–371.

Charpak, S., Mertz, J., Beaurepaire, E., Moreaux, L., and Delaney, K. (2001). Odor-evoked calcium signals in dendrites of rat mitral cells. Proc. Natl. Acad. Sci. USA *98*, 1230–1234.

Chuhma, N., and Ohmori, H. (2002). Role of Ca(2+) in the synchronization of transmitter release at calyceal synapses in the auditory system of rat. J. Neurophysiol. *87*, 222–228.

Cuttle, M.F., Tsujimoto, T., Forsythe, I.D., and Takahashi, T. (1998). Facilitation of the presynaptic calcium current at an auditory synapse in rat brainstem. J. Physiol. *512*, 723–729.

Delaney, K.R., and Tank, D.W. (1994). A quantitative measurement of the dependence of short-term synaptic enhancement on presynaptic residual calcium. J. Neurosci. *14*, 5885–5902.

Duchen, M.R. (1986). Excitation of mouse motoneurones by GABA-mediated primary afferent depolarization. Brain Res. *379*, 182–187.

Dudel, J. (1971). The effect of polarizing current on action potential and transmitter release in crayfish motor nerve terminals. Pflugers Arch. *324*, 227–248.

Felmy, F., and Schneggenburger, R. (2004). Developmental expression of the Ca2+-binding proteins calretinin and parvalbumin at the calyx of held of rats and mice. Eur. J. Neurosci. *20*, 1473–1482.

Felmy, F., Neher, E., and Schneggenburger, R. (2003). Probing the intracellular calcium sensitivity of transmitter release during synaptic facilitation. Neuron *37*, 801–811.

Forsythe, I.D., Tsujimoto, T., Barnes-Davies, M., Cuttle, M.F., and Takahashi, T. (1998). Inactivation of presynaptic calcium current contributes to synaptic depression at a fast central synapse. Neuron *20*, 797–807.

Grynkiewicz, G., Poenie, M., and Tsien, R.Y. (1985). A new generation of Ca2+ indicators with greatly improved fluorescence properties. J. Biol. Chem. *260*, 3440–3450.

Habets, R.L., and Borst, G.J. (2005). Post-tetanic potentiation in the rat calyx of Held synapse. J. Physiol. *564*, 173–187.

Helmchen, F., Borst, J.G., and Sakmann, B. (1997). Calcium dynamics associated with a single action potential in a CNS presynaptic terminal. Biophys. J. *72*, 1458–1471.

Hubbard, J.I., and Willis, W.D. (1968). The effects of depolarization of motor nerve terminals upon the release of transmitter by nerve impulses. J. Physiol. *194*, 381–405.

Iwasaki, S., and Takahashi, T. (1998). Developmental changes in calcium channel types mediating synaptic transmission in rat auditory brainstem. J. Physiol. *509*, 419–423.

Jackson, M.B., and Redman, S.J. (2003). Calcium dynamics, buffering, and buffer saturation in the boutons of dentate granule-cell axons in the hilus. J. Neurosci. *23*, 1612–1621.

Jang, I.S., Jeong, H.J., Katsurabayashi, S., and Akaike, N. (2002). Functional roles of presynaptic GABA(A) receptors on glycinergic nerve terminals in the rat spinal cord. J. Physiol. *541*, 423–434.

Kamiya, H., and Zucker, R.S. (1994). Residual Ca2+ and short-term synaptic plasticity. Nature *371*, 603–606.

Kaneko, M., and Takahashi, T. (2004). Presynaptic mechanism underlying cAMP-dependent synaptic potentiation. J. Neurosci. *24*, 5202–5208.

Khakh, B.S., and Henderson, G. (2000). Modulation of fast synaptic transmission by presynaptic ligand-gated cation channels. J. Auton. Nerv. Syst. *81*, 110–121.

Kim, M.-H., Korogod, N., Schneggenburger, R., Ho, W.-K., and Lee, S.-H. (2005). Interplay between Na+/Ca2+ exchangers and mitochondria in Ca2+ clearance at the calyx of Held. J. Neurosci. *25*, 6057–6065.

Kobayashi, K., and Tachibana, M. (1995). Ca2+ regulation in the presynaptic terminals of goldfish retinal bipolar cells. J. Physiol. *483*, 79–94.

Korogod, N., Lou, X., and Schneggenburger, R. (2005). Presynaptic Ca2+ requirements and developmental regulation of posttetanic potentiation at the calyx of Held. J. Neurosci. *25*, 5127–5137.

Lou, X., Scheuss, V., and Schneggenburger, R. (2005). Allosteric modulation of the presynaptic Ca2+ sensor for vesicle fusion. Nature *435*, 497–501.

MacDermott, A.B., Role, L.W., and Siegelbaum, S.A. (1999). Presynaptic ionotropic receptors and the control of transmitter release. Annu. Rev. Neurosci. *22*, 443–485.

Maeda, H., Ellis-Davies, G.C., Ito, K., Miyashita, Y., and Kasai, H. (1999). Supralinear Ca2+ signaling by cooperative and mobile Ca2+ buffering in Purkinje neurons. Neuron *24*, 989–1002.

Matveev, V., Sherman, A., and Zucker, R.S. (2002). New and corrected simulations of synaptic facilitation. Biophys. J. *83*, 1368–1373.

Matyushkin, D.P., Krivoi, I.I., and Drabkina, T.M. (1995). Synaptic feed-backs mediated by potassium ions. Gen. Physiol. Biophys. *14*, 369–381.

Meinrenken, C.J., Borst, J.G., and Sakmann, B. (2002). Calcium secretion coupling at calyx of Held governed by nonuniform channel-vesicle topography. J. Neurosci. *22*, 1648–1667.

Nicholls, J., and Wallace, B.G. (1978). Modulation of transmission at an inhibitory synapse in the central nervous system of the leech. J. Physiol. *281*, 157–170.

Regehr, W.G., Delaney, K.R., and Tank, D.W. (1994). The role of presynaptic calcium in short-term enhancement at the hippocampal mossy fiber synapse. J. Neurosci. *14*, 523–537.

Rosenmund, C., Sigler, A., Augustin, I., Reim, K., Brose, N., and Rhee, J.S. (2002). Differential control of vesicle priming and short-term plasticity by Munc13 isoforms. Neuron *33*, 411–424.

Sakaba, T., and Neher, E. (2001a). Calmodulin mediates rapid recruitment of fast-releasing synaptic vesicles at a calyx-type synapse. Neuron *32*, 1119–1131.

Sakaba, T., and Neher, E. (2001b). Quantitative relationship between transmitter release and calcium current at the calyx of Held synapse. J. Neurosci. *21*, 462–476.

Schneggenburger, R., and Neher, E. (2000). Intracellular calcium dependence of transmitter release rates at a fast central synapse. Nature *406*, 889–893.

Shapiro, E., Castellucci, V.F., and Kandel, E.R. (1980). Presynaptic membrane potential affects transmitter release in an identified neuron in Aplysia by modulating the Ca2+ and K+ currents. Proc. Natl. Acad. Sci. USA *77*, 629–633.

Smith, C., Moser, T., Xu, T., and Neher, E. (1998). Cytosolic Ca2+ acts by two separate pathways to modulate the supply of release-competent vesicles in chromaffin cells. Neuron *20*, 1243–1253.

Takeuchi, A., and Takeuchi, N. (1961). Changes in potassium concentration around motor nerve terminals, produced by current flow, and their effects on neuromuscular transmission. J. Physiol. (Paris) *155*, 46–58.

Takeuchi, A., and Takeuchi, N. (1962). Electrical changes in pre- and postsynaptic axons of the giant synapse of Loligo. J. Gen. Physiol. *45*, 1181–1193.

Tang, Y., Schlumpberger, T., Kim, T., Lueker, M., and Zucker, R.S. (2000). Effects of mobile buffers on facilitation: experimental and computational studies. Biophys. J. *78*, 2735–2751.

Turecek, R., and Trussell, L.O. (2001). Presynaptic glycine receptors enhance transmitter release at a mammalian central synapse. Nature *411*, 587–590.

Turecek, R., and Trussell, L.O. (2002). Reciprocal developmental regulation of presynaptic ionotropic receptors. Proc. Natl. Acad. Sci. USA *99*, 13884–13889.

Voets, T., Neher, E., and Moser, T. (1999). Mechanisms underlying phasic and sustained secretion in chromaffin cells from mouse adrenal slices. Neuron *23*, 607–615.

Wang, L.Y., and Kaczmarek, L.K. (1998). High-frequency firing helps replenish the readily releasable pool of synaptic vesicles. Nature *394*, 384–388.

Wojtowicz, J.M., and Atwood, H.L. (1984). Presynaptic membrane potential and transmitter release at the crayfish neuromuscular junction. J. Neurophysiol. *52*, 99–113.

Wu, L.G., and Borst, J.G. (1999). The reduced release probability of releasable vesicles during recovery from short-term synaptic depression. Neuron *23*, 821–832.

Wu, L.G., Borst, J.G., and Sakmann, B. (1998). R-type Ca2+ currents evoke transmitter release at a rat central synapse. Proc. Natl. Acad. Sci. USA *95*, 4720–4725.

Yamada, W.M., and Zucker, R.S. (1992). Time course of transmitter release calculated from simulations of a calcium diffusion model. Biophys. J. *61*, 671–682.

Ye, J.H., Wang, F., Krnjevic, K., Wang, W., Xiong, Z.G., and Zhang, J. (2004). Presynaptic glycine receptors on GABAergic terminals facilitate discharge of dopaminergic neurons in ventral tegmental area. J. Neurosci. *24*, 8961–8974.

Zucker, R.S., and Regehr, W.G. (2002). Short-term synaptic plasticity. Annu. Rev. Physiol. *64*, 355–405.